

Switchable Genetic Oscillator Operating in Quasi-Stable Mode

Natalja Strelkova and Mauricio Barahona

Department of Bioengineering & Institute for
Mathematical Sciences,
Imperial College London,
South Kensington Campus, London SW7 2AZ,
United Kingdom

Abstract

Ring topologies of repressing genes have qualitatively different long-term dynamics if the number of genes is odd (they oscillate) or even (they exhibit bistability). However, these attractors may not fully explain the observed behavior in transient and stochastic environments such as the cell. We show here that even repressilators possess quasi-stable, travelling-wave periodic solutions that are reachable, long-lived and robust to parameter changes. These solutions underlie the sustained oscillations observed in even rings in the stochastic regime, even if these circuits are expected to behave as switches. The existence of such solutions can also be exploited for control purposes: operation of the system around the quasi-stable orbit allows us to turn on and off the oscillations reliably and on demand. We illustrate these ideas with a simple protocol based on optical interference that can induce oscillations robustly both in the stochastic and deterministic regimes.

Key words: synthetic biology; oscillatory gene networks; generalized repressilator; traveling waves; stochastic dynamics

Introduction

Recent experimental advances in cellular and molecular biology have made it possible to engineer intricate gene regulatory circuits (1). Inspired in many cases by electronic elements, simple gene networks

have been designed to perform reproducible, low-level functions. Some classic examples include the toggle switch (2), the genetic ring oscillator known as the repressilator (3), or a circuit that can exhibit both oscillatory and switching behavior through the alteration of biochemical interactions (4). Such simple circuits could be potentially interconnected and built-up to form more elaborate ‘biological devices’ with large numbers of components. This trend is facilitated by simulation software containing large number of genes (5) as well as libraries of composable biological parts for experimental realization (6). Simple synthetic modules can also be integrated into the complex machinery of the cell, as in the oscillator recently implemented in a mammalian cell (7), or interfaced with cellular pathways to induce particular responses, as in the construct where the toggle switch was connected to the SOS pathway to induce DNA protection mechanisms in *E. coli* when exposed to UV light (8). Similar principles have been exploited in the rational design of internal negative feedback operated in conjunction with external arabinose-driven positive feedback to produce cell-synchronized oscillations (9).

The central role played by oscillations in cellular function has made oscillatory circuits a primary target for the analysis and design of synthetic networks. A particular area of interest is the elucidation of strategies leading to robust timing and sequential activation in the cell. For instance, key stages in developmental biology and in cell differentiation may be controlled by so-called master regulators—a small set of transcription factors sequentially activating and driving several other genes with accurate timing (10, 11, 12). In addition, studies of both natural (13, 14) and engineered circuits (15) indicate that the correct timing and order of gene activation is a key characteristic of balanced, optimal cell function, as it reduces the metabolic burdening that ensues from the continuous presence of heterologous substances (16).

In this paper, we consider the dynamics and control of noisy genetic oscillatory circuits in quasi-stable mode operation. We exemplify our results with one of the simplest and most widely studied synthetic networks: the N -gene ring repressilator (Fig. 1*a*). Some natural networks of master regulators (10) contain

such ring structures as subnetworks, making the exploration of their dynamic behavior relevant for both naturally occurring and synthetic systems. The underlying idea is well-known: when observing the dynamics of systems operating in highly variable environments, such as the cell, it might not be enough to characterize only the long-term attractors of the system since unstable solutions can play a significant role. For instance, quasi-stable transients might be so long-lived as to be the most significant feature of the observed noisy dynamics (17). Moreover, the presence of noise in nonlinear systems may induce non-stationary dynamics in systems with only fixed point attractors in the deterministic setting (18) or, conversely, noise may act as a stabilizer of unstable deterministic states (19).

In the generalized repressilator, results due to Smith (20, 21) show that rings with an even number of genes (e.g., the toggle switch (2) with $N = 2$) exhibit multistability and hence behave like switches in the stochastic regime. On the other hand, rings with an odd number of genes (like the standard repressilator (3) with $N = 3$) have a globally attracting limit cycle and are therefore oscillators both in the stochastic and deterministic regimes. However, we show here that generalized repressilators possess an intricate structure of unstable periodic orbits that play an important part in their observable noisy and transient dynamics. In particular, even rings have a quasi-stable limit cycle which, although unstable in terms of linear Floquet stability analysis, has only one unstable direction with a very slow escape rate. This means that trajectories are attracted to the limit cycle from all directions but one, hence leading to long-lived, inducible periodic transients in the deterministic setting and to sustained oscillations in the stochastic system. These effects become more pronounced as the number of genes grows. Therefore the finite-time, observable noisy dynamics of an even repressilator ring is not necessarily static (switch-like) but rather exhibits oscillatory characteristics.

In addition to their effect on the observable dynamics, quasi-stable oscillatory modes can be used as operating points to control the system around them. The advantage of such a scheme is that the oscillations can be switched on and off, unlike limit cy-

cle attracting behavior. Operation around unstable modes, usually illustrated with the example of the inverted pendulum (22), is a classic scenario in control theory for enhanced controllability and speed of response. It has a long and successful history of applications in fluid flow control (23) and in the steering of jet aircraft (24). Here, we illustrate the application of this concept to gene networks with a simple protocol of controlled interference based on an optical mechanism for readout and induction of gene expression. Our simulations show that even repressilator rings in quasi-stable operation behave as a robust and on-demand switchable oscillator in which genes become upregulated periodically in an ordered sequence according to a travelling-wave solution. This characteristic, which is robust at high and low copy numbers, could be used for synthetic biological applications such as accurately timed interference with naturally occurring networks.

Theory

Model equations and stability of fixed points

The generalized repressilator consists of a ring of N genes in which transcription of each gene is repressed by the product of the preceding gene (Fig. 1a). A deterministic model of this circuit is given by the following set of ordinary differential equations:

$$\begin{aligned} \dot{m}_i &= \frac{c_1}{1 + p_{i-1}^2} - c_2 m_i \\ \dot{p}_i &= c_3 m_i - c_4 p_i, \end{aligned} \quad (1)$$

where p_i and m_i describe protein and mRNA concentrations for each gene, respectively (3). Here, $i = 1, \dots, N$ with the periodic boundary condition $p_0 = p_N$, and c_1 (c_3) is the creation rate and c_2 (c_4) is the degradation rate for the mRNAs (proteins). The production of mRNA is modeled as a source term that depends nonlinearly on the concentration of the inhibitor protein. Proteins are assumed to be produced at a rate linearly dependent on the amount of the corresponding mRNA. The degradation of mRNA and proteins is assumed to be linearly proportional to their current amount. The toggle switch (2) and

the repressilator oscillator (3), which have both been implemented in *E. coli*, are special cases with $N = 2$ and $N = 3$, respectively. Based on analytical results on monotone systems due to Smith (20, 21), the stability analysis of this circuit reveals a fundamental difference between rings with odd and even numbers of genes. We briefly sketch some of the main results, which are also summarized in Fig. 1b.

The stability analysis characterizes the long-term dynamic behaviors of the deterministic system. An example of such behavior is given by the fixed points of the system, i.e., the states in which the dynamics is stationary. The variation of a parameter can produce a change in the stability or the existence of fixed points or other attractors. This is called a bifurcation and it leads to qualitative changes in the long-term behavior of the system. One can find the parameter values at which bifurcations are produced by performing a bifurcation analysis, which can be carried out analytically (in some simple cases) or numerically with the aid of continuation software packages such as AUTO (25), which can also track the stability of periodic solutions.

In our system (1), the fixed points, where all derivatives are zero, are found from the condition:

$$p_i^* \left(1 + p_{i-1}^*\right)^2 = \frac{c_1 c_3}{c_2 c_4} \equiv c, \quad \forall i. \quad (2)$$

The parameter c defined in Eq. (2) will play the role of the bifurcation parameter for even rings. A positive and real solution is obtained if all proteins have the same concentration: $p_i^* = p_{i+1}^* = p_m, \forall i$ and

$$p_m = \left[\frac{c}{2} + \sqrt{\frac{c^2}{4} + \frac{1}{27}} \right]^{\frac{1}{3}} - \frac{1}{3} \left[\frac{c}{2} + \sqrt{\frac{c^2}{4} + \frac{1}{27}} \right]^{-\frac{1}{3}}.$$

This solution, which exists as long as c is positive, is stable for small c and becomes unstable for larger values of c in both odd and even rings.

In the case of even rings, a pitchfork bifurcation takes place at $c = 2$ for all N . The two additional stable fixed points arising at that value of the parameter correspond to $p_i^* = p_{i+2}^* \neq p_{i+1}^*, \forall i$, which

gives:

$$\begin{aligned} p_i^* &= \frac{c}{2} + \sqrt{\frac{c^2}{4} - 1} \equiv p_u \\ p_{i+1}^* &= \frac{c}{2} - \sqrt{\frac{c^2}{4} - 1} \equiv p_d. \end{aligned} \quad (3)$$

Note that $p_u \rightarrow c - 1/c$ and $p_d \rightarrow 1/c$ for large c . The new fixed points of the system (1) correspond to two distinct dimerized states: one in which genes with odd indices are upregulated (p_u) while genes with even indices are downregulated (p_d); and another symmetric state where the genes with odd and even indices exchange their patterns of regulation. These solutions are equivalent to tiling the ring with copies of the steady state solution of the two-gene ring, and are similar to other dimerized degenerate solutions in classic models of conjugated polymers and spin chains (26). Therefore, after the bifurcation, the system is bistable, i.e, it behaves like a switch in the presence of noise.

In the case of odd rings, p_m becomes unstable following a bifurcation that occurs at a value $c(N)$ that approaches 2 as N grows. However, in this case the bifurcation is Hopf: no additional fixed points appear but rather the bifurcation signals the emergence of a periodic solution. Smith (20) proved that in monotone systems (i.e., systems in which partial derivatives do not change sign) such as the repressilator, the periodic solution that emerges is a globally attracting stable limit cycle. Therefore odd rings behave as stable oscillators following the Hopf bifurcation.

Floquet theory and unstable periodic orbits

The stability analysis presented above does not provide information about unstable periodic solutions. Although, in principle, unstable periodic orbits are not relevant for the long-term deterministic dynamics, they can be key to the observed dynamics, especially if the orbits involve slow time scales. Such *quasi-stable oscillations* can appear as transients in deterministic simulations and are likely to be observed in the corresponding stochastic simulations. In fact, it was in numerical simulations that we first noticed the relevance of these modes in even repressilator rings.

Floquet theory can be used to find periodic solutions and quantify their linear stability in terms of their Poincaré map, i.e., the crossings of the orbit with a (hyper)plane in phase space. Under this analysis, a periodic solution (a closed orbit) becomes a fixed point of the Poincaré map and its stability is reformulated as the linear stability of this fixed point. The eigenvalues of the Poincaré map linearized around the fixed point constitute the Floquet multipliers. They indicate how an infinitesimal perturbation around the orbit decays or grows (exponentially). The periodic solution is linearly stable if all the Floquet multipliers have magnitudes smaller than unity (see the Supplementary Material for references and details on Floquet Theory). In some cases, a few (possibly only one) Floquet multipliers will be slightly larger than one. We will then have 'quasi-stable' periodic solutions in that it takes a long time to diverge away from them. Quasi-stability in this sense is a local property. To assess if these solutions will be reachable (and therefore observable in the dynamics), one needs to employ global techniques, e.g. sampling the space of initial conditions. However, Floquet analysis provides an indication of the possibility of observable, yet unstable, periodic solutions. If a periodic orbit has a small number of very weakly unstable directions, it is likely that it could be observed as long-lived periodic transients in the deterministic system and that it could also play a role in the stochastic dynamics. Moreover, such quasi-stable orbits are good candidates for a control mechanism that can induce oscillations on demand, as shown below.

Methods

Numerical simulations and analysis of the dynamics

The deterministic system of ODEs (1) was solved numerically with an adaptive fourth-order Runge-Kutta integrator (27), in which the step-size automatically adapts to meet the required accuracy ϵ . We have checked that the inducibility, reachability and transient times of the quasi-stable oscillations are not af-

ected by the accuracy of the integrator by using the Runge-Kutta integrator with accuracies ϵ between 10^{-2} and 10^{-8} (see Supplementary Material for details). In addition, the observability of the unstable orbits was confirmed by using a nonlinear integrator (28).

The bifurcation analysis and the calculation of the Floquet multipliers of the unstable periodic orbits were carried out with the numerical continuation software AUTO (25) (see *Supplementary Material*).

Stochastic simulations of the generalized repressilator were performed using the classical Gillespie algorithm (29). Random numbers and quasi-random numbers for numerical simulations were generated with the GSL Scientific Library (30).

Global robustness analysis and control aspects of quasi-stable oscillations

As part of our numerical evaluation of the generalized repressilator, we have developed a method to carry out a robustness and reachability analysis of its quasi-stable oscillations. This was necessary because available global robustness tools (28) quantify changes in fixed points induced by parameter variations and are therefore not directly applicable to oscillations. In order to evaluate the global robustness and inducibility of the quasi-stable oscillations, we attempt to induce sustained oscillations with a predetermined intervention and quantify changes in the observed response when the model parameters are varied. The method defines an operating point in parameter space (the reference set c_i^*), based on biologically appropriate estimates, and a hypercube around it to account for biological variability, temperature gradients and other noise. We then sample parameter sets from the hypercube using Reverse Halton Sequences (31), quasi-random sequences that have been shown to converge faster than standard Monte Carlo sampling for high dimensional spaces (2). For each sampled parameter set, we attempt to induce oscillations with the STOP-KICK scenario described below and record if the system evolves towards sustained oscillations. If oscillations are observed, we calculate numerically the period of the oscillation and the change in shape (see supplementary material for

details). Characterizing the change in shape is essential to establish that the oscillation remains detectable and functionally recognizable in the biological system. Note that here we are only concerned with global robustness of the reachability of the solution. A modification of the same algorithm could be used to study the parameter combinations that contribute most strongly to the sensitivity of the network, a question relevant for the experimental tuning of the system that is not addressed here.

Results

Stable and quasi-stable oscillations in the generalized repressilator

As pointed out in the Theory section, odd repressilator rings are globally attracted to stable limit cycle oscillations for $c > 2$. Numerical simulations show that the period of these solutions increases linearly with the number of genes in the ring (Fig. 2*a*). The stability analysis also shows that, in contrast, even rings only support fixed points as stable solutions. However, direct dynamical simulations of even repressilator rings reveal the existence of long-lived periodic solutions, which are easily reachable, as checked by extensive sampling (not shown) of the space of initial conditions. The period of these oscillations also increases linearly with the number of genes, albeit with a slope that is approximately half of that in odd rings (Fig. 2*a*).

These numerical observations do not pose a contradiction with the stability analysis above: the observed oscillations in even rings are periodic solutions yet unstable. Unstable solutions can be studied using the numerical bifurcation detection software AUTO (25), a continuation package that does not rely on dynamical simulations (see Supplementary material). We have used AUTO to find bifurcations in the biologically relevant range of the parameter c and to assess the linear stability of fixed points and periodic solutions—the latter through Floquet analysis.

The result for even rings is presented in Table 1. In agreement with the analytical results, a pitchfork

bifurcation is found numerically as a branching point at $c = 2$, above which Hopf bifurcations leading to the appearance of unstable periodic solutions are detected in all rings with more than 4 genes. The Floquet stability analysis indicates that the first unstable periodic orbit to emerge has only one unstable direction, regardless of the number of genes. The only positive Floquet multiplier, which indicates how fast the trajectory diverges away from the orbit, is small and decreases as the length of the ring increases. This is the signature of quasi-stability: if this periodic orbit is reached, it will be long-lived. We have also checked that this solution is reachable through numerical sampling of the space of initial conditions (see Supplementary material). Such reachable quasi-stable modes affect significantly the observed transient dynamics and also play a central role in stochastic dynamics where unstable solutions are explored under the effect of noise. Both these conditions are relevant for dynamics of genetic circuits inside the cell.

The existence of quasi-stable modes provides us with the opportunity to design a distinct control strategy. If we control the system to revolve around a quasi-stable mode, the result is an oscillator that can be switched on, kept oscillating and switched off on demand. Below, we introduce a simple implementation of such a scenario and evaluate its robustness of operation. Note that an intricate family of unstable periodic orbits with high symmetry exists both in odd and even rings (see Table 1 and Supplementary Material). However, these additional periodic solutions have several unstable directions that make them essentially unobservable and uncontrollable.

Spatio-temporal structure of the periodic solutions

The spatio-temporal structure of the periodic solutions, both in the odd and even cases, corresponds to a travelling-wave solution propagating around the ring. The snapshots in Figs. 2*b,c* show that this propagation occurs against the backdrop of the dimerized fixed point solution of the even ring, where all odd (even) numbered genes are ‘up’ while the even (odd) numbered genes are ‘down’ (3). Clearly, a dimerized

configuration cannot be accommodated in an odd ring. This leads to a kink-like (frustrated) solution where two consecutive genes have similar expression levels. This local imbalance of repression induces a dynamical instability that makes the kink propagate around the odd ring in a periodic fashion (Fig. 2*b*). This spatio-temporal structure underlies the limit cycle solution in odd rings. The fact that the period of the limit cycle increases (roughly) linearly with the number of genes indicates that the speed of propagation of the kink is (roughly) constant.

The quasi-stable periodic solution in even rings can be interpreted under the same prism. Figure 2*b* shows that it corresponds to *two interacting kinks* propagating around the ring at a roughly constant speed with a period that is approximately one half of that of the closest odd ring (Fig. 2*a*). The instability of this periodic solution has a clear meaning in this picture: if the two kinks ‘collide’, they annihilate each other and the system returns to the stable fixed point, i.e., the dimerized solution. Figure 2*b* also shows that each kink has a minimum spatial width that depends on the parameters of the model. Hence it is more difficult to find these oscillatory solutions in rings that are not large enough to fit two such perturbations although they can still be observed in smaller, biologically realizable rings (see Supplementary material). For clarity, we have chosen to illustrate the spatio-temporal structure of the solutions with long rings. However, we have checked that the quasi-stable periodic orbits in rings with $N = 6, 8, 10$ (not shown) maintain the features of the two-kink-structure and operate under the same principles as the long rings shown in Fig. 2*b*.

The spatio-temporal structure of the periodic solutions in repressilator rings shows a strong parallelism with similar dynamical solutions observed in classical models of discrete lattices (33). The travelling-wave nature of the oscillations could have potential biological applicability if one were to use this circuit as a control element for genes that must be activated in a particular order and for a pre-defined time interval.

Robust induction of quasi-stable oscillations in the deterministic regime

The causal constraints imposed by the travelling-wave structure means that the manipulation of one gene will have a predictable effect on the others. This property can be used to induce and stop oscillations in even rings reliably by activation of one gene for a short time span. We illustrated this simple scenario in Fig. 3*a*. First, the even ring is forced to converge to one of the fixed point solutions with a STOP signal that consists of the external activation of gene j for a time interval longer than the period of the oscillation. This signal is used to ‘initialize’ the system, suppressing any transient oscillations present in the system. Once the system is at rest, the oscillation can be started with a KICK signal, consisting of the external activation of gene $j + 1$ with a step function of width and amplitude similar to those of the oscillatory pattern. Such signals can be imparted non-invasively through an optical mechanism that uses UV or red light to activate the production of mRNAs of particular genes (34, 35).

In order to check that the proposed protocol is robust to parameter variations, we have carried out a global robustness analysis as outlined in the Methods section. We construct a hypercube by taking variations of 5%, 10% and 20% around the reference values of the parameters in Eq. (1) and take 10^4 samples in this hypercube varying all parameters simultaneously. Sampling is performed with quasi-random Reverse Halton Sequences for improved convergence (2, 31). Figure 3*b* shows that the fraction of parameter samples that lead to oscillations with this protocol converges to 1 for large rings. Our numerics also show that oscillations can be elicited with significant robustness in rings with $N > 6$. When oscillations are present, the period shows very small variation with respect to the reference set, as shown by the coefficient of variation (Fig. 3*b*, inset). We have also quantified the change in the shape of oscillations through a normalized mean square measure and found that the shapes in the perturbed system exhibit very high similarity ($\approx 99\%$) to the reference set (see Supplementary material). In summary, our global robustness analysis indicates that in the deter-

ministic regime, long-lived quasi-stable periodic solutions are reliably inducible in larger rings with a single intervention. For moderate size rings, oscillations can still be induced for a large fraction of the parameter hypercube but are shorter lived. This suggests that repeated interventions could be used in order to keep the ring in the quasi-stable oscillating state. A simple control protocol that implements these ideas is proposed in the following section and shown to be applicable for rings as small as $N = 6$ operating in the stochastic regime.

Stochastic oscillations in even rings and readout-based control

We have used the standard Gillespie algorithm (29) to study the generalized repressilator in the stochastic regime, i.e., when intrinsic noise is high due to low copy numbers. It is well known that stochastic models of odd rings behave as oscillators and that the travelling wave structure is preserved (3, 36). In the case of even rings, we have performed long stochastic simulations (not shown) and found bistability and switching events, as expected from the long-term attractors of the underlying deterministic system. Additionally, the simulations show sustained oscillatory behavior, especially in longer rings although they are also observable in rings as small as $N = 6$ (see Supplementary material). The oscillations appear in a variety of settings: as transients from a variety of initial conditions; spontaneously emerging from one of the stable points; or associated with switching events. It is also easy to induce such oscillations with localized interventions in particular genes; to sustain them with periodic driving; and to terminate them with a prolonged induction of a gene (as in the STOP signal above). We have examined the structure of these oscillations and they correspond well with the quasi-stable periodic solutions in the deterministic system: their period is approximately half the period of the closest odd ring (Fig. 2a) and the spatio-temporal travelling-wave structure is maintained.

Our numerical simulations confirm the relevance of the underlying quasi-stable oscillations for the observed stochastic dynamics of even rings. Similarly to the deterministic case, the quasi-stable mode can

also be used as a control operating point such that the system becomes switchable. The robust reachability of this mode allows us to use an extremely simplified feedback mechanism that could be implemented through an optical read-out (GFP, YFP or luciferase protein labeling) and response (on-demand UV or red light gene transcription activation) (34). The simple control scheme illustrated in Fig. 4a uses the optical read-out from two successive proteins in the ring to introduce optical KICK signals that sustain the oscillation based on a threshold rule (Fig. 4b). The oscillation can be started and terminated using the same optical signals. Although we have chosen to illustrate the possible implementation of the control scheme with light sensitive inducers, it is worth remarking that any suitable mechanism capable of precisely-timed gene induction with good spatial resolution at the cell population could be used. A potential advantage of this switchable mode of operation is the economical and targeted use of the transcriptional resources without overburdening the cell with unnecessary mRNA production (16).

Discussion

In this work, we have studied how the presence of quasi-stable periodic solutions affects the observable dynamics of even repressilator rings. Previously, even rings have been thought of as switches due to the fact that they only support fixed point solutions. However, our bifurcation analysis reveals the existence of a set of unstable orbits, some of which have slow timescales associated with them. These quasi-stable periodic solutions are both reachable and long-lived, thus playing a role in the observed dynamics, both transient and stochastic. This suggests that oscillatory behavior might be more widespread than expected in genetic models since it could feature in systems that possess only static attractors.

The presence of quasi-stable solutions provides us with the possibility of designing control protocols that operate the system around such modes so that the oscillations can be turned on and off reliably. Our numerics indicate that a robust mechanism could be implemented based on appropriate optical feed-

back to switch the system between stable fixed points and quasi-stable oscillations. Although the proposed pared-down control scheme is only intended to provide an illustration of the potential implementation and its performance could be improved with the use of optimized strategies for stochastic and robust control that take into account specific details of the experimental setup, it is worth discussing some of its limitations. The challenge for the dynamical control algorithm is to deliver the optical interference signal necessary for the induction of gene expression for a short time period, to a particular spatial area of the cell population, and with a well-controlled delay following the fluorescent signal of the proteins. The proposed scheme shows both enough spatial and time resolution to address individual cells in a population with well-defined pulses (34). The scheme would need to rely on proper calibration of life-times of fluorescent proteins affected by phototoxic and photobleaching effects, as reviewed in detail by Bennett and Hasty (37). Finally, since the delay between the actual protein concentration and the corresponding fluorescent signal introduced by the maturation time ($\sim 2-8$ min) is short compared to the period of the oscillation (~ 130 min), this would be acceptable for the control scheme.

A synthetic circuit operating under such principles could be interfaced with a naturally occurring network to induce an intrinsic interference that is interruptible on-demand. The switchability of this regulatory element can help avoid the appearance of adverse cumulative effects. The NF κ B pathway is an example where such a regulator could provide controlled activation over short time intervals as an alternative to conventional knock-downs and other functional interventions that modify the balance of important proteins for the cell cycle (38, 39). The underlying traveling wave structure of the observed periodic solutions could also be potentially useful for design purposes. It allows for coordinated intervention when the timing and order of activation of different pathways is crucial. Examples of cellular networks, e.g. in developmental biology, indicate that timed patterns of sequential activation are at the heart of the function of families of master regulators (11, 14, 42, 43) and, in the case of the vertebrate segmentation clock (40, 41),

the associated oscillations are well-defined but do not survive in the long-term. The importance of heterogeneously timed gene induction has also been highlighted in a model of Arabinose uptake in *E. coli* (13). Experiments with genetically engineered yeast have also shown that pulsed activation of chaperons followed by pulsed activation of the associated heterologous proteins is more efficient at maximizing the production of particular metabolites (16). These applications hint at potential uses for circuits that can produce sequential patterns of activation on demand, such as the even repressilator studied here, which interact with other cellular pathways via intrinsic proteins, thus avoiding the timed delivery of external agents through the cell membrane.

The design of control strategies for the operation of systems around an inherently unstable state has a long history in other disciplines (e.g., flight and fluid control) since it affords enhanced responsiveness and controllability with relative ease and simplicity of design (22). This strategy differs fundamentally from the biochemical alteration of the network topology proposed by Atkinson et al. (4) based on a smaller gene circuit but with a complex regulatory scheme involving promoter and repressor sites regulating one gene. The molecular kinetics of such regulators are less well understood than those with single regulatory sites due to unavoidable cross-talk and compound logic. The ring topology relies on simple regulation to provide a sequence of causal signals but at the expense of involving a larger number of genes.

The present scheme is also in contrast with previously engineered gene circuits, such as odd repressilators, which possess globally attracting limit cycles leading to behavior that is robust yet not controllable. Quasi-stable operation, on the other hand, is robustly switchable. The switchability of the oscillator coupled with dynamic control that affords good spatial resolution could be used to elicit localized oscillations in cell populations as an aid to examine mechanisms of cell synchronization. It is an open area of current research to elucidate the role of a design concept based on control around unstable behavior, similar to the inverted pendulum in classic control theory, to further our understanding of cell strategies and its potential use in the design of synthetic

topologies that can interfere with naturally occurring pathways.

Acknowledgements

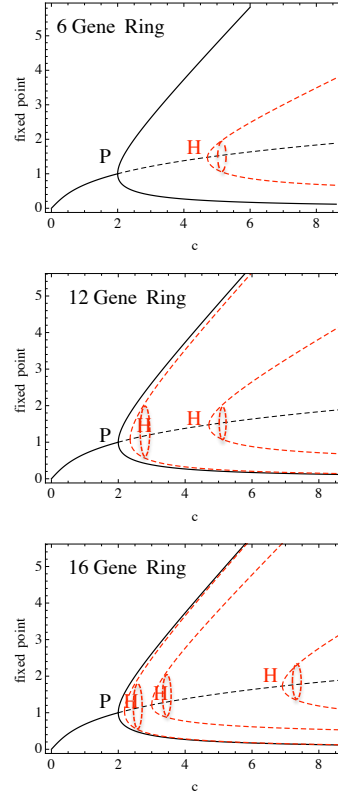
N.S. gratefully acknowledges support from the Wellcome Trust through grant 080711/Z/06/Z. We thank Manos Drakakis, Karen Polizzi, Andreas Ipsen and Tomasz Leja for inspiring discussions and suggestions.

References

1. Andrianantoandro, E., S. Basu, D. K. Karig, and R. Weiss, 2006. Synthetic biology: new engineering rules for an emerging discipline. *Mol. Sys. Bio.* 2:2006.0028.
2. Gardner, T., C. R. Cantor, and J. J. Collins, 2000. Construction of a genetic toggle switch in *Escherichia coli*. *Nature* 403:339–342.
3. Elowitz, M. B., and S. Leibler, 2000. A synthetic oscillatory network of transcriptional regulators. *Nature* 403:335–338.
4. Atkinson, M. R., M. A. Savageau, J. T. Myers, and A. J. Ninfa, 2003. Development of Genetic Circuitry Exhibiting Toggle Switch or Oscillatory Behavior in *Escherichia coli*. *Cell* 113:597–607.
5. Marchisio, M., and J. Stelling, 2008. Computational design of synthetic gene circuits with composable parts. *Bioinformatics* 24:1903–1910.
6. MIT Registry. <http://partsregistry.org>. Accessed June 6, 2009 .
7. Tigges, M., T. T. Marquez-Lago, J. Stelling, and M. Fussenegger, 2009. A tunable synthetic mammalian oscillator. *Nature* 457:309–312.
8. Kobayashi, H., M. Kaern, M. Araki, C. K., T. S. Gardner, C. R. Cantor, and J. J. Collins, 2004. Programmable cells: interfacing natural and engineered gene networks. *Proc. Natl. Acad. Sci. USA* 101:8414–8419.
9. Stricker, J., S. Cookson, M. R. Bennett, W. H. Mather, L. S. Tsimring, and J. Hasty, 2008. A fast, robust and tunable synthetic gene oscillator. *Nature* 456:516–519.
10. Borneman, A. R., J. A. Leigh-Bell, H. Yu, P. Bertone, M. Gerstein, and M. Snyder, 2006. Target hub proteins serve as master regulators of development in yeast. *Genes Dev.* 20:435–448.
11. Liu, Y., M. Asakura, H. Inoue, T. Nakamura, M. Sano, Z. Niu, M. Chen, R. J. Schwartz, and M. D. Schneider, 2007. Sox17 is essential for the specification of cardiac mesoderm in embryonic stem cells. *Proc. Natl. Acad. Sci. USA* 104:3859–3864.
12. Bondue, A., G. Lapouge, C. Paulissen, C. Semeraro, M. Iacovino, M. Kyba, and C. Blanpain, 2008. Mesp1 Acts as a Master Regulator of Multipotent Cardiovascular Progenitor Specification. *Cell Stem Cell* 3:69–84.
13. Megerle, J. A., G. Fritz, U. Gerland, K. Jung, and J. O. Rädler, 2008. Timing and Dynamics of Single Cell Gene Expression in the Arabinose Utilization System. *Biophys. J* 95:2103–2115.
14. Spencer, S. L., S. Gaudet, J. G. Albeck, J. M. Burke, and P. K. Sorger, 2009. Non-genetic origins of cell-to-cell variability in TRAIL-induced apoptosis. *Nature* 459:428–432.
15. Glick, B. R., 1995. Metabolic load and heterologous gene expression. *Biotechnology Advances* 13:247 – 261.
16. Glieder, A., 2009. Technische Universität Graz. Private Communication .
17. Trefethen, L. N., and M. Embree, 2005. Spectra and pseudospectra. Princeton University Press, Princeton, NJ, USA.
18. Süel, G. M., J. Garcia-Ojalvo, L. M. Liberman, and M. B. Elowitz, 2006. An excitable gene regulatory circuit induces transient cellular differentiation. *Nature* 440:545–550.
19. Turcotte, M., J. Garcia-Ojalvo, and G. M. Süel., 2008. A genetic timer through noise-induced stabilization of an unstable state. *Proc. Natl. Acad. Sci. USA* 105:15732–15737.
20. Smith, H., 1987. Oscillations and multiple steady states in a cyclic gene model with repression. *J. Math. Biol.* 25:169–190.

21. Müller, S., J. Hofbauer, L. Endler, C. Flamm, S. Widder, and P. Schuster, 2006. A generalized model of the repressilator. *J. Math. Biol.* 53:905–937.
22. Franklin, G. F., A. Emami-Naeini, and J. D. Powell, 1993. Feedback Control of Dynamic Systems. Addison-Wesley Longman Publishing Co., Inc., Boston, MA, USA.
23. Ahuja, S., and C. W. Rowley, 2009. Feedback control of unstable steady states of flow past a flat plate using reduced-order estimators arXiv.org:0902.1207.
24. McRuer, D., and D. Graham, 2004. Flight Control Century: Triumphs of the Systems Approach. *J. of Guidance, Control, and Dynamics* 27:161–173.
25. Doedel, E., 2007. AUTO 07. Software for Continuation and Bifurcation Problems in Ordinary Differential Equations .
26. Soos, Z., 2007. Identification of dimerization phase transitions driven by Peierls and other mechanisms. *Chemical Physics Letters* 440:87–91.
27. Press, W. H., S. A. Teukolsky, W. T. Vetterling, and B. P. Flannery, 1992. Numerical recipes in C: the art of scientific computing. Cambridge University Press, 2 edition.
28. Zi, Z., Y. Zheng, A. E. Rundell, and E. Klipp, 2008. SBML-SAT: a systems biology markup language (SBML) based sensitivity analysis tool. *BMC Bioinformatics* 9.
29. Gillespie, D. T., 1977. Exact Stochastic Simulation of Coupled Chemical Reactions. *J. Chem. Phys.* 8:2340–2361.
30. Galassi, M., J. Davies, J. Theiler, B. Gough, G. Jungman, P. Alken, M. Booth, and F. Ross. GNU Scientific Library Reference Manual. 3 (v1.12) edition.
31. Halton, J., 1960. On the efficiency of certain quasi-random sequences of points in evaluating multi-dimensional integrals. *Numer. Math.* 2 84–90.
2. Vandewoestyne, B., and R. Cools, 2006. Good permutations for deterministic scrambled Halton sequences in terms of L2-discrepancy. *J. Comput. Appl. Math.* 189:341–361.
33. Braun, O., and Y. Kivshar, 2004. The Frenkel-Kontorova Model. Concepts, Methods, and Applications. Springer, illustrated edition.
34. Shimizu-Sato, S., E. Huq, J. M. Tepperman, and P. H. Quail, 2002. A light-switchable gene promoter system. *Nat. Biotech* 20:1041–1044.
35. Levskaya, A., A. A. Chevalier, J. J. Tabor, Z. B. Simpson, L. A. Lavery, M. Levy, E. A. Davidson, A. Scouras, A. D. Ellington, E. M. Marcotte, and C. A. Voigt, 2005. Synthetic biology: engineering Escherichia coli to see light. *Nature* 438:441–2.
36. Hemberg, M., and M. Barahona, 2007. Perfect Sampling of the Master Equation for Gene Regulatory Networks. *Biophys. J.* 93:401–410.
37. Bennett, M. R., and J. Hasty, 2009. Microfluidic devices for measuring gene network dynamics in single cells. *Nat Rev Genet* 10:628–638.
38. Karin, M., and A. Lin, 2002. NF- κ B at the crossroads of life and death. *Nat Immunol* 3:221–227.
39. Naugler, W. E., and M. Karin, 2008. NF- κ B and cancer - identifying targets and mechanisms. *Current Opinion in Genetics & Development* 18:19–26.
40. Yun-Jin, B. L. Aerne, L. Smithers, C. Haddon, D. Ish-Horowicz, and J. Lewis, 2000. Notch signalling and the synchronization of the somite segmentation clock. *Nature* 408:475–479.
41. Pourquie, O., 2003. The Segmentation Clock: Converting Embryonic Time into Spatial Pattern. *Science* 301:328–330.
42. Ashall, L., C. A. Horton, D. E. Nelson, P. Paszek, C. V. Harper, K. Sillitoe, S. Ryan, D. G. Spiller, J. F. Unitt, D. S. Broomhead, D. B. Kell, D. A. Rand, V. See, and M. R. H. White, 2009. Pulsatile Stimulation Determines Timing and Specificity of NF-kappaB-Dependent Transcription. *Science* 324:242–246.
43. Holtzendorff, J., D. Hung, P. Brende, A. Reisenauer, P. H. Viollier, H. H. McAdams, and L. Shapiro, 2004. Oscillating Global Regulators Control the Genetic Circuit Driving a Bacterial Cell Cycle. *Science* 304:983–987.

N	Bifurcation	c	Stable/all directions	Max. Floquet	Period (min)
2	BP	2.00	-	-	-
4	BP	2.00	-	-	-
6	BP	2.00	-	-	-
	HB	4.68	11/12	6.2	132
8	BP	2.00	-	-	-
	HB	3.00	15/16	3.9	186
10	BP	2.00	-	-	-
	HB	2.56	19/20	3.0	239
	HB	9.62	17/20	9.0	104
12	BP	2.00	-	-	-
	HB	2.36	23/24	2.5	291
	HB	4.68	21/24	6.2	132
14	BP	2.00	-	-	-
	HB	2.24	27/28	2.2	342
	HB	3.51	25/28	4.8	160
	HB	16.9	23/28	10.5	94
16	BP	2.00	-	-	-
	HB	2.18	31/32	2.0	393
	HB	3.00	29/32	3.9	186
	HB	6.91	27/32	7.8	113
18	BP	2.00	-	-	-
	HB	2.15	35/36	1.8	444
	HB	2.71	33/36	3.4	213
	HB	4.71	31/36	6.2	132
	HB	27.33	29/36	11.5	89



Bifurcation analysis and unstable periodic solutions of repressilator rings with even number of genes.

We use the continuation package AUTO (25) to obtain the bifurcations of rings of size N (1). The parameter c , defined in Eq. (2), is swept in the biologically relevant range $c \in [0.001, 30]$ by changing c_1 with $c_2 = 0.12$, $c_3 = 0.16$ and $c_4 = 0.06$ constant. In agreement with analytical calculations, a branching point (P), corresponding to a pitchfork bifurcation, is found at $c = 2$. A series of Hopf bifurcations (HB) linked to the emergence of unstable periodic solutions are found subsequently. Floquet analysis indicates that the first unstable orbit to emerge has only one unstable direction, regardless of the dimension of the system, and that the maximal Floquet multiplier decreases with increasing N . Hence this periodic solution is quasi-stable: if it is reached, the divergence away from it is slow, and gets slower for longer rings. Other unstable orbits are present but their high instability makes them irrelevant to the observed dynamics. A similar structure of unstable orbits exists in odd rings (see Supplementary Material). The figure on the right shows the bifurcation diagrams for even rings of length $N = 6, 12, 16$. The unstable periodic orbits, shown in red dashed lines, emerge through Hopf bifurcations.

Figure Legends

Figure 1. Attractors of the generalized repressilator model

(a) Topology of the generalized repressilator: N genes in a cycle where each gene is repressed by the protein product of the preceding gene. Also shown is the reaction scheme underlying the dynamical system (1) with production and degradation terms for the mRNA (m_j) and protein (p_j) of each gene. The repression of the production of mRNA is modelled by a Hill-type term $H(p_{j-1})$. (b) Typical time traces of the long-term deterministic dynamics of an odd ring and an even ring above the bifurcation point $c = 2$: odd rings converge to a globally attracting periodic solution while even rings converge to fixed points. The time traces shown correspond to $N = 23$ and $N = 22$. (c) Stability of the fixed points of the system as a function of the bifurcation parameter c . Even rings undergo a pitchfork bifurcation at $c = 2$, leading to the emergence of two stable fixed points. Odd rings undergo a Hopf bifurcation leading to the emergence of a limit cycle. The critical parameter for the Hopf bifurcation depends on N but tends to $c = 2$ as N grows (see Supplementary material).

Figure 2. Periodic solutions and travelling waves in the generalized repressilator model

(a) The period of the limit cycle of the deterministic model of odd rings (solid line) increases linearly with the length of the ring. Simulations of the stochastic version of this system using the Gillespie algorithm show that the period (shown as circles) follows the same trend, although they are slightly larger. The period of the quasi-stable solutions found in even rings (deterministic and stochastic) increases linearly with the number of genes but with a slope that is half that of the odd rings. The inset shows representative time traces of the periodic solutions in odd rings (stable) and in even rings (quasi-stable). (b) Time snapshot of the spatial distribution of the concentrations of two successive proteins concentrations for the periodic solution in the odd ring with $N = 23$. The solution has a travelling-wave structure with a kink-like perturbation propagating around the ring, indicated by the arrow in the bottom figure. The bottom figure represents the minimum distance $|\Delta p_j| = \min(|p_u - p_j|, |p_d - p_j|)$ between

the traveling wave solution and the dimerized solution with an alternating pattern of protein expression given by p_u and p_d . The distance becomes large around the kink in the traveling wave solution. (c) Same as (b) for the quasi-stable periodic solution of the even ring with $N = 22$. In this case, the travelling wave solution has two kinks that propagate around the ring, as indicated by the arrows.

Figure 3. Robust induction of oscillations in even rings in the deterministic regime

(a) The quasi-stable periodic solution in even repressilator rings can be induced with a simple sequence of signals. First, apply a STOP signal to gene j to force the system to approach a fixed point solution. Second, apply a KICK signal to gene $j + 1$ to drive the ring into oscillation. The oscillation can be terminated at will by applying another STOP signal. The signals can be implemented via on-demand UV or red light gene transcription activation (34). This STOP-KICK-STOP protocol is shown here for a ring with $N = 18$ with parameters $c_1 = 2.6$, $c_2 = 0.12$, $c_3 = 0.2$, $c_4 = 0.06$. (b) Global robustness analysis of the inducibility of the quasi-stable oscillations. The STOP-KICK scenario is applied to 10^4 random combinations of parameters c_i for each even ring of length N and we record the proportion of parameter sets that lead to five oscillations. The parameters are sampled with reverse Halton sequences from a hypercube with 5% (■), 10% (●) and 20% (◆) variation around the reference set. Quasi-stationary oscillations are robustly induced for $N \geq 10$, while smaller rings can be kept in the oscillating state applying repeated interventions in a simple control protocol as shown in Fig. 4. (Inset) The oscillations are robust in shape (not shown) and in period to changes in the parameters. The relative variability (coefficient of variation) of the period of the induced oscillations is small and decreases with the length of the ring.

Figure 4. Stochastic oscillations in even rings and readout-based control.

(a) Illustration of the readout-based control scheme for a ring of 6 genes. Two proteins of the ring are read out with fluorescent tags. This readout is then compared to a

reference defined according to the oscillating behavior of the ring, with similar period and a shift between consecutive genes. The reference comparison is threshold-based and leads to an ON-OFF (1-0) control for the KICK signals. These can be implemented with light responsive genes promoters. In the numerical simulations shown in (b), the KICK signals are indicated with the red markings in the upper panels. (b) A simple readout-based control reliably switches on the oscillations, sustains them and switches them off. The control mechanism functions by monitoring two successive proteins in the ring. Whenever each of them falls below a threshold, a KICK signal for the corresponding protein is given. These threshold-based KICK signals are indicated with red and magenta markings in the upper panels. The oscillation can be terminated with a STOP signal as in the deterministic state. The optical read-out can be based on GFP or YFP protein labeling while the response can be implemented with on-demand UV or red light that enhances the production of the corresponding mRNAs (34). The figure shows the application of this mechanism to a ring with $N = 10$. The stochastic time traces correspond to the protein expression of proteins p_j with $j = 1, 3, 5, 7, 9$ and the corresponding control (top) in response to proteins p_1 and p_2 (trace not shown). The right figure is a magnification of the dashed square inside the main figure. We have also checked that this control protocol is applicable for rings with as low as $N = 6$ genes (not shown).

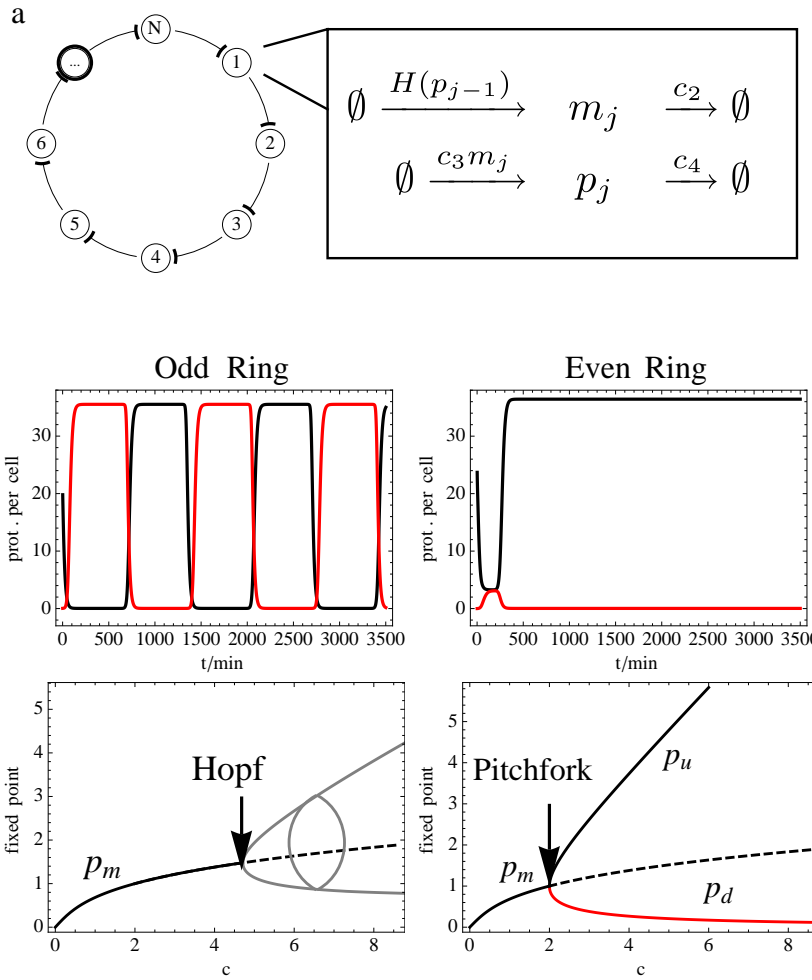


Figure 1:

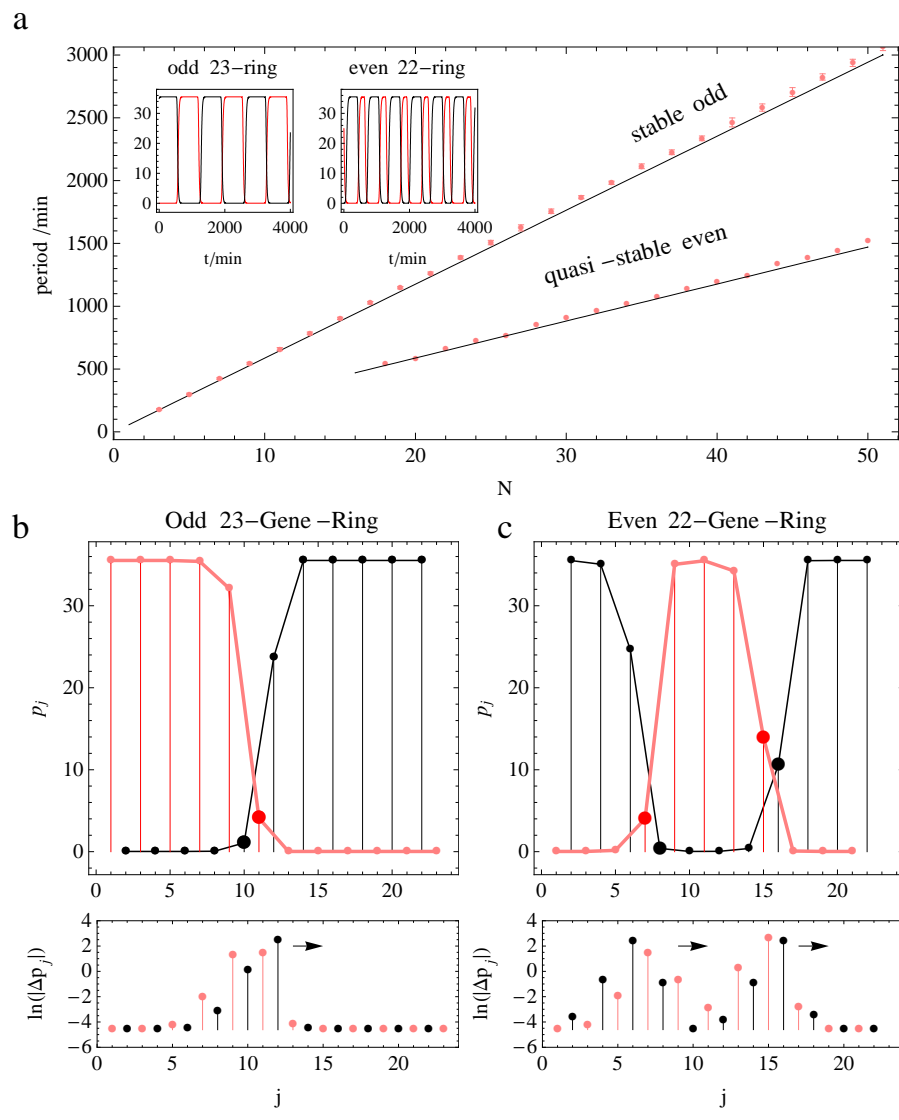


Figure 2:

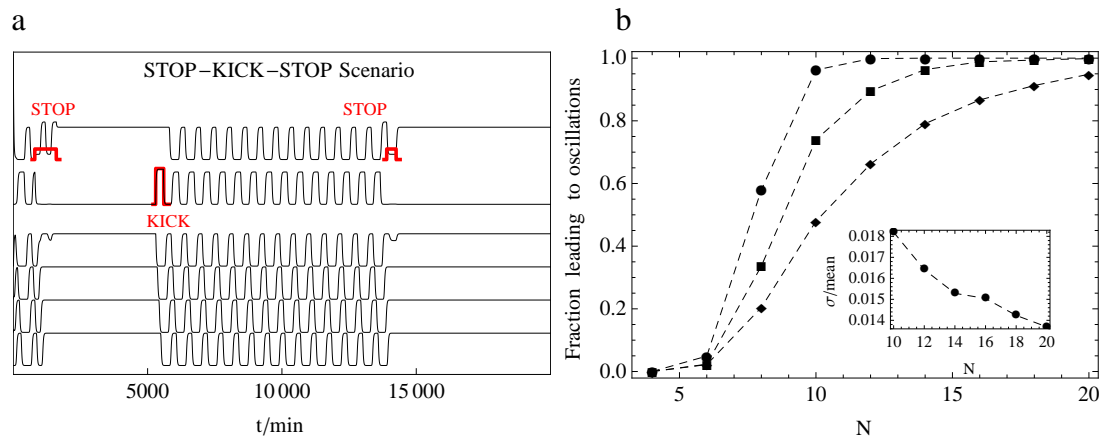


Figure 3:

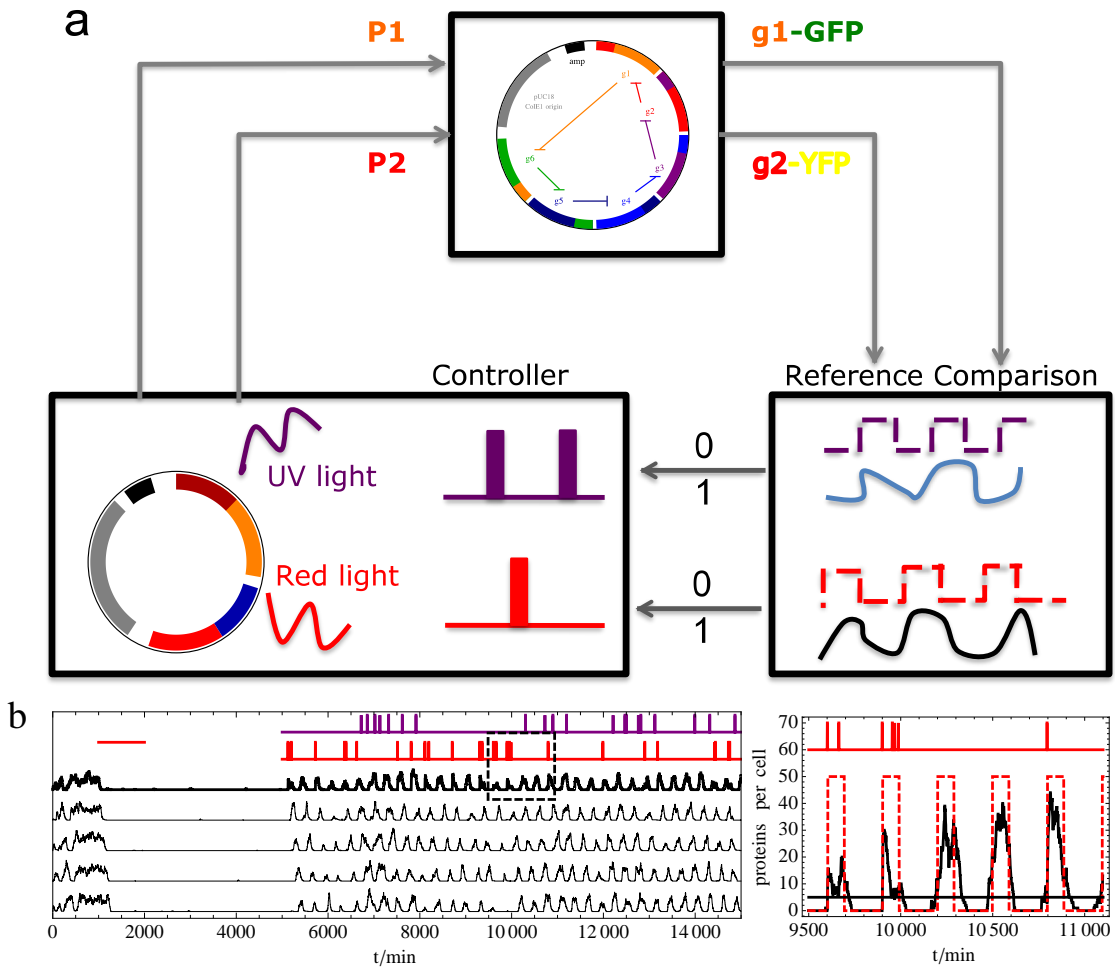


Figure 4:

Supplementary Material

1 Stability analysis and bifurcations in odd and even rings

N	Bifurcation	c	Stable/all directions	Max. Floquet	Period (min)
3	HB	4.689	6/6	1	132
5	HB	2.556	10/10	1	239
7	HB	2.244	14/14	1	342
	HB	16.91	12/14	8.0	94
9	HB	2.156	18/18	1	444
	HB	4.711	16/18	5.0	132
11	HB	2.089	22/22	1	545
	HB	3.311	20/22	3.75	169
	HB	42.84	18/22	11.0	86
13	HB	2.067	26/26	1	645
	HB	2.800	24/26	3.05	204
	HB	7.778	22/26	7.55	110
15	HB	2.044	30/30	1	746
	HB	2.533	28/30	2.63	239
	HB	4.711	26/30	5.76	132
17	HB	2.044	34/34	1	847
	HB	2.400	32/34	2.35	274
	HB	3.667	30/34	4.68	154
	HB	11.75	28/34	9.13	100

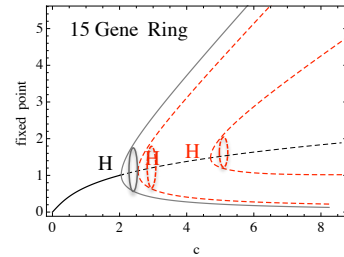
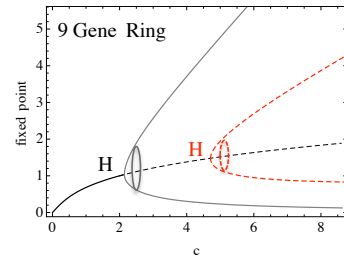
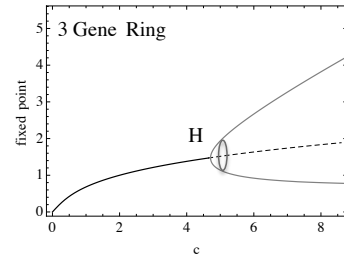


Table SM1: Bifurcation analysis of repressilator rings with odd number of genes and corresponding bifurcation diagrams.

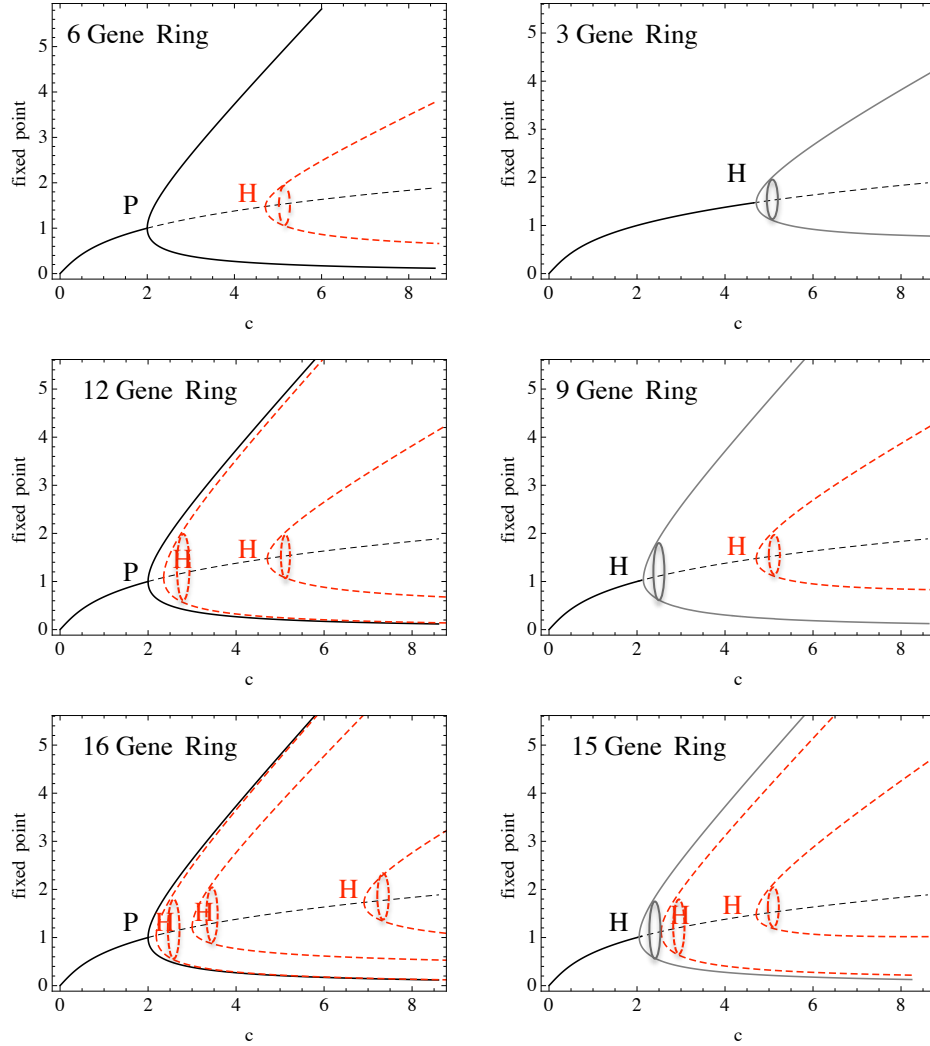


Figure 5: Bifurcation diagrams for odd and even case. The unstable periodic orbits are shown in red dashed lines. As the number of genes in the ring increases the first unstable orbit moves towards stable structures (stable fixed points for the even rings and stable limit cycles for the odd rings. This suggests that the first unstable orbits may become more observable in larger rings. The sampling of initial condition space shown below confirms this hint.)

Table SM1 and Figure 5 summarize the result of our analysis using AUTO to obtain the bifurcations of odd rings of size N . As in the main text, the parameter c is swept in the biologically relevant range $c \in [0.001, 30]$. In agreement with analytical calculations summarized in the main text, a series of Hopf

bifurcations (HB) are found. The first one leads to a stable limit cycle, whose maximum Floquet multiplier is 1 corresponding to the trivial direction along the orbit. The subsequent bifurcations give birth to unstable periodic orbits with an increasing number of unstable directions (always even). These unstable orbits are essentially irrelevant to the observed dynamics because they are highly unstable and not reachable. The relationships between the periods of oscillations in rings of different lengths hints at a strong symmetry in the spatio-temporal structure of these solutions. We summarize the findings in Table SM1 and Figure 5.

2 Basic Floquet Theory and Quasi-Stable Oscillating Orbits under Noise

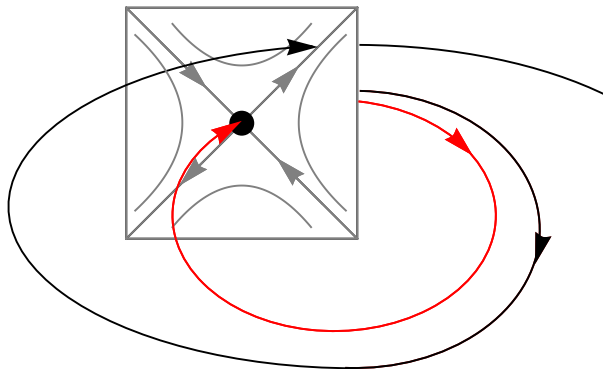


Figure 6: Poincaré map with quasi-stable fixed point (black) and possible trajectories. The periodic orbit (red trajectory) is linearly stable along the left diagonal, where the arrows are pointing towards the fixed point and unstable along the right diagonal, where the arrows are pointing away from the fixed point. The escape scenario from unstable periodic orbit due to perturbations is illustrated with black trajectory.

As pointed out in the main text we have observed long lasting oscillations in the even rings randomly sampling the initial condition space. The observed oscillating modes can be assessed regarding their stability with the Floquet Multipliers theory (3). Here, the question about stability of the orbit can be reformulated to the question for the stability of the corresponding fixed point x^* in the Poincaré map. If v_0 is an infinitesimal perturbation such that $x^* + v_0$ is in S , then after the first return to S

$$x^* + v_1 = P(x^* + v_0) \approx P(x^*) + [DP(x^*)]v_0 \quad (4)$$

The Eigenvalues λ_j of the linearized Poincaré map $[DP(x^*)]$ obtained this way are nontrivial Floquet multipliers. The closed orbit is linearly stable if and only if $|\lambda_j| < 1$ for all j . We illustrate the case where the closed orbit has unstable directions and how the system may escape from it in Figure 6 above. The Poincaré section (shown in gray) has stable directions (left diagonal) and unstable directions (right diagonal). The system may escape the closed orbit (black trajectory) in a directed manner once perturbed along the unstable direction.

Since it is a biological system it is important to show that the quasi-stable orbits are observable under noise effects. We can simulate small biological noise effects using less accurate integration with larger maximal

error ϵ per step (see "Methods" section in the main text). This is in addition to the robustness analysis under parameter variations illustrated in Figure **SS1**. It turns out that the oscillations do not become less robust and last as long as with the accurate integration.

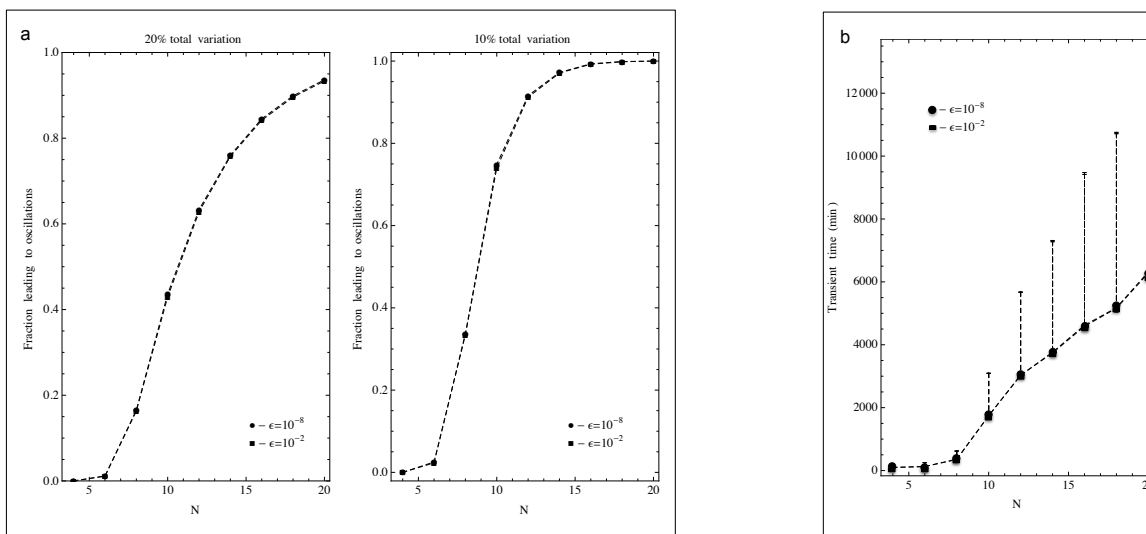


Figure SS1: **a** Robustness of STOP-KICK-STOP scenario as illustrated in the main text Figure 3a. The accuracy control parameter ϵ for circles is 10^{-2} , whereas in the main text the parameter was 10^{-8} . Both curves are for the same total variation. Comparing the result to the main text, we see that less accurate integration does not change the robustness of the STOP-KICK-STOP scenario significantly. Less accurate integration is a way to simulate the biological noise and these quasi-stable oscillations do not become significantly less robust under the noise simulated with less accurate integration as shown here and also simulated with Gillespie algorithm as shown later in the control scheme in the main text. (See the paragraph below for the intuitive explanation for this phenomenon.) **b** Different accuracy also does not significantly affect the length of transient oscillations, which die off within a certain period of time (for instance within 50 oscillations). The figure illustrates the mean lengths of oscillations, which occur if starting from the randomly chosen initial condition and inspect the region for 50 oscillations. The error bars are first and third quartiles.

We try to give an intuitive explanation for the observed effect. Errors resulting from less accurate integration affect all variables describing protein and mRNA concentrations. It has the effect that the system is perturbed in all directions due to this noise. However, the generalized repressilator system can escape the oscillating orbit through directed movement along one out of many possible directions (see Figure 6 above and Table 1 in the main text). If the system is perturbed along other directions, it is pulled back to the limit cycle, because all other directions are attractive. Therefore random perturbations do not necessarily kill the transient oscillations. On the contrary, random perturbations may interfere with the directed escape out of the limit cycle and this might even stabilize the oscillations. In fact in the following section we show fluctuations due to internal noise stabilize the oscillations.

3 Sampling of Initial Condition Space and Spontaneous Transient Oscillations in the Stochastic Setting

The bifurcation analysis revealed the existence of quasi-stable periodic solutions in the generalized repressilator model. However, it is not clear if these solutions are observable under random sampling of the initial condition space. Here we show for the deterministic setting how often on average a randomly sampled initial condition can lead to at least 5, 10, and as many as 50 oscillations Fig. 7.

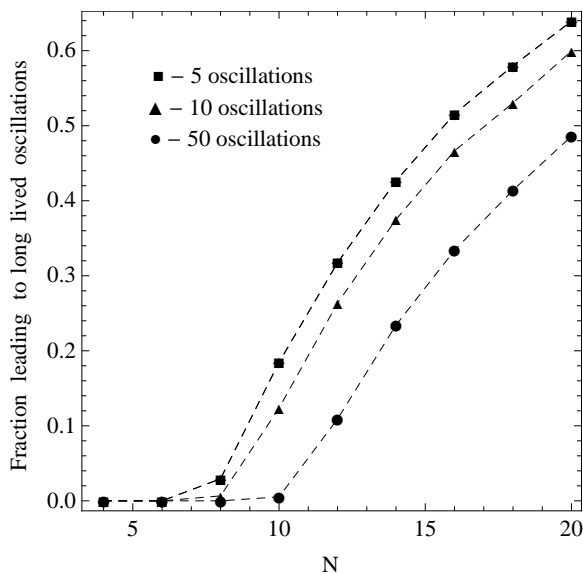


Figure 7: Sampling of the initial condition space for the deterministic simulations. The initial condition hyper cube defined as 0 to maximal amplitude (Note: the maximal amplitude of the proteins is not the same as the maximal amplitude for the mRNAs) has been sampled 10^4 times using pseudo random numbers (reverse Halton sequences).

In the stochastic setting the noise due to small copy numbers does not destroy the oscillations in the even rings. On the contrary, this is also how we have discovered these modes. The quasi-stable structure identified with the deterministic bifurcation theory becomes even more prevalent under internal noise. So, in this case noise does actually excite the oscillations. The following parameters have been used $c_1 = 1.6$, $c_2 = 0.12$, $c_3 = 2.6$, $c_4 = 0.06$. The picture shows that in the stochastic regime the system spontaneously goes into the oscillating state more frequently than the equivalent deterministic description. The initial conditions for the stochastic simulation are chosen to be the same as in the deterministic case and 10 runs for each starting value has been collected.

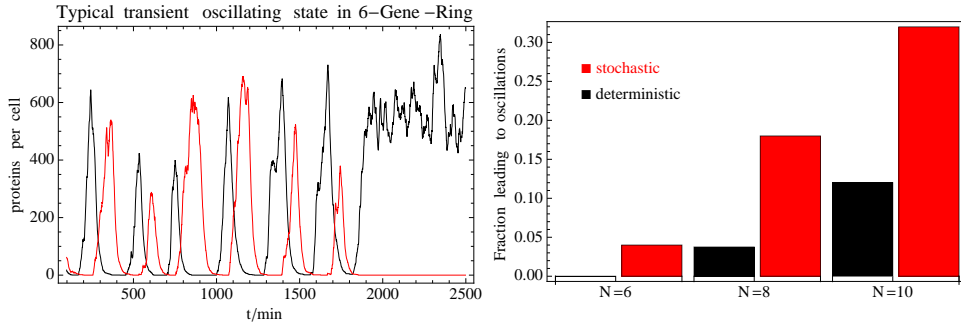


Figure 8: Transient oscillations are more prevalent in the stochastic setting. For the same initial conditions and the same constants the system goes more frequently into the oscillating state than in the deterministic setting.

4 Robustness Analysis and Shape Similarity

We perform global robustness analysis, which means all parameters are varied at the same time within specified multidimensional hypercube. If we want to obtain a global robustness of let say 10 gene ring, then the dimension of the according parameter space would be 40, there are 4 constants for each gene (c_1, c_2, c_3, c_4) and these are varied independently of each other. This procedure is fundamentally different to standard robustness assessments, where only one parameter is gradually varied at the same time.

The parameter hypercube is created as 5%, 10%, 20% variation around the reference state, where all parameters c_i are the same for all the genes. We sample this parameter hypercube in an efficient manner using pseudo-random numbers created with reverse Halton sequences. This sampling of large dimensional space with pseudo-random numbers was shown to be more efficient than the classical MC (2). After selecting a set of parameters in this way, we evolve the system in time first applying the STOP signal, which puts it into stationary up/down solution. Then we apply a KICK scenario and record if the oscillations have persisted for at least 5 periods. The requirement here is that all genes have shown a non decaying amplitude. In this way we obtain 10^4 samples for each gene number and plot the fraction of the samples leading to the oscillations on the y-Axes.

In addition to the 0,1 decision on if or not the fraction oscillates we quantify the change in the shape of the oscillation. This is independent of the variation in period and amplitude. The measure *ssh* would give large dissimilarity scores if the oscillations would become spiky, the gene being in the up state is much smaller than being in the down state or vice versa. It would give intermediate scores if instead of being rather quadratic, it becomes like a Gaussian shape. Mathematically, we first scale the time for the reference shape and for the perturbed system shape to 1. Through the scaling we get rid of the variations in the period lengths. Then we apply the standard normalized L_2 -norm,

$$ssh = \frac{\langle \pi_{ref}(t) \pi_{pert}(t) \rangle}{\langle \pi_{ref}(t) \rangle \langle \pi_{pert}(t) \rangle} \quad (5)$$

where the normalization scales away the differences in the amplitude. This measure assesses shape changes for moderate parameter perturbations and gives an additional information to the variation in the oscillation amplitude and period length.

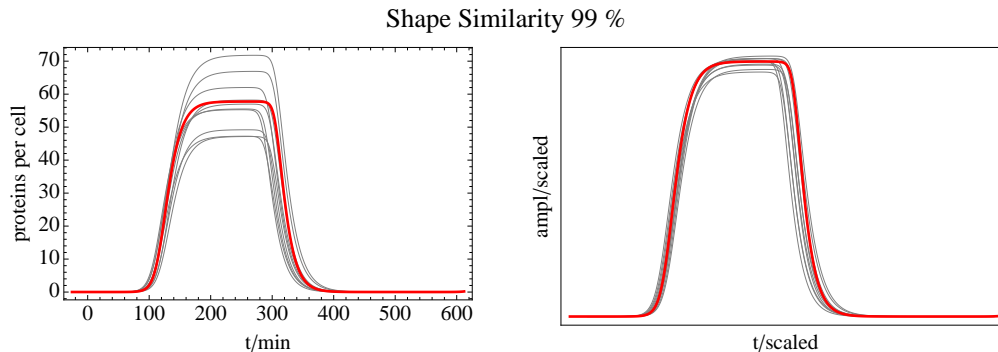


Figure 9: Shape variations under the global parameter changes. On the left we see the numerically observed oscillations, which differ moderately in the period length and amplitude. The reference shape for the unperturbed system is shown in red. On the right the time scale (x-Axis) has been scaled with the period and the maximal amplitude for each curve respectively. This demonstrates how the scaling in time and normalized L_2 score assesses the shape similarity.

5 Bifurcation Software AUTO

AUTO (4) performs systematic variation of specified parameters and assessment of qualitative characteristics of ODE system such as fixed points, periodic orbits and their stability. The ODEs are of the form:

$$u'(t) = f(u(t), p), \quad f(\cdot, \cdot), u(\cdot) \in R^n \quad (6)$$

The limited bifurcation analysis is done by solving algebraic equations

$$f(u, p) = 0, \quad f(\cdot, \cdot), u \in R^n \quad (7)$$

One of the limitations of the package is that the continuation must start nearby guessed/known stable fixed point. If such starting point is given, when solution branches are calculated as one or more parameters are gradually changed.

For our system there is a regime, where only one stable fixed point exists (see the Theory section in the main text). Starting from that equilibrium point we have performed the continuation gradually changing one parameter and identified the bifurcation points.

References

1. N. G. van Kampen (2007) *Stochastic Processes in Physics and Chemistry*. 3-rd Edition. (Elsevier, Amsterdam)
2. B. Vandewoestyne and R. Cools (2006) Good permutations for deterministic scrambled Halton sequences in terms of L2-discrepancy *J. Comput. Appl. Math.* 189:341–361
3. S. H. Strogatz (1994) *Nonlinear Dynamics and Chaos*. (Westview Press)
4. E Doedel (2007) AUTO 07. Software for Continuation and Bifurcation Problems in Ordinary Differential Equations